Adaptive Image Interpolation Based on Local Gradient Features

Jung Woo Hwang and Hwang Soo Lee, *Member, IEEE*

***Abstract*—This letter presents two adaptive interpolation methods based on applying an inverse gradient to conventional bilinear and bicubic interpolation. In simulations, the proposed methods exhibited a better performance than conventional bilinear and bicubic methods, particularly in the edge regions. In addition, the proposed methods can be used irrespective of the magnification factor (MF) and easily implemented due to their simple structure.**

***Index Terms*—Image interpolation, image reconstruction.**

I. Introduction

CONVENTIONAL linear image interpolation schemes (e.g., bilinear and bicubic schemes) are popular and widely used due to their computational simplicity. However, such methods have a serious blurring problem, particularly in edge regions. Since the blurring is due to a nonadaptive interpolation structure, this letter proposes efficient and good quality interpolation algorithms using an adaptive approach.

Various algorithms have already been developed to solve the problem of blurring based on an adaptive approach [1]–[7]. However, with multiresolution pyramid-based techniques [1]–[3] and edge-directed interpolation techniques [4]–[6], the magnification factor (MF) is normally limited to a power of two. This is because multiresolution pyramid formulations, such as those using a Laplacian pyramid and wavelet, are based on the interrelation between the upper and lower images, while edge-directed interpolation formulations are based on the continuity of edges. Although [7] does not have such a limitation and uses nearest neighbor and one-dimensional (1-D) bilinear interpolation adaptively according to the edge direction along with pre- and postfiltering, the performance of its own adaptive interpolation algorithm has not been demonstrated.

Accordingly, this letter proposes efficient and good quality interpolation algorithms with an arbitrary MF based on the use of an inverse gradient. The application of an inverse gradient to the structure of conventional bilinear and bicubic interpolation produces better results as regards the peak signal-to-noise ratio (PSNR) and a perceptual image comparison. More detail will be given in the description of adaptive bilinear (A-bilinear) and bicubic (A-bicubic) interpolation. The basic motivation comes from [8], where an inverse gradient is used as an enhanced way of solving the demosaic problem, i.e., finding missing colors in a color filter array, in a digital still camera.

Manuscript received December 9, 2002; revised April 27, 2003. The associate editor coordinating the review of this manuscript and approving it for publication was Dr. Ricardo L. de Queiroz.

The authors are with the Department of Electrical Engineering and Computer Science, Korea Advanced Institute of Science and Technology (KAIST), Seoul 130-012, Korea (e-mail: jwhwang66@mail.kaist.ac.kr).

Digital Object Identifier 10.1109/LSP.2003.821718

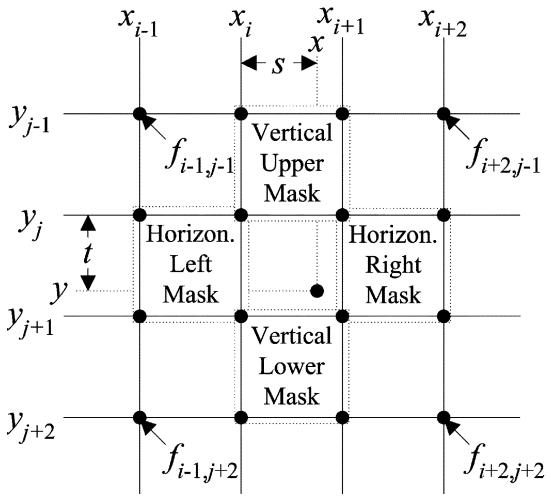

Fig. 1. Masks for inverse gradient weights.

II. A-Bilinear Interpolation

In the following formulation, f is a two-dimensional (2-D) array of the input digital image, G is a function of the two variables representing the interpolation function, and g is a 2-D array of the output digital image. The output digital image is represented by

$$g_{k,l} = G\left(\frac{k}{r}, \frac{l}{r}\right) \tag{1}$$

where r is the MF and k and l are the pixel positions. When (x, y) is a point in the rectangular subdivision $[x_i, x_{i+1}] \times [y_j, y_{j+1}]$ in Fig. 1, the 2-D bilinear interpolation function G_{bil} is given as

$$\begin{aligned} G_{\text{bil}}(x,y) = (1-t)\left((1-s)f_{i,j} + sf_{i+1,j}\right) \\ +t\left((1-s)f_{i,j+1} + sf_{i+1,j+1}\right) \end{aligned} \tag{2}$$

where $s = x - x_i$, $t = y - y_i$.

In general, images interpolated by the conventional bilinear and bicubic interpolation are blurred as a result of ignoring the local features of the images. As shown in (2), the weights of each input image pixel is only a function of the distances s and t shown in Fig. 1. However, in addition to distance, the weights should also intuitively depend on the local features of the image, so as to obtain a better reconstructed image quality. Fig. 2 shows

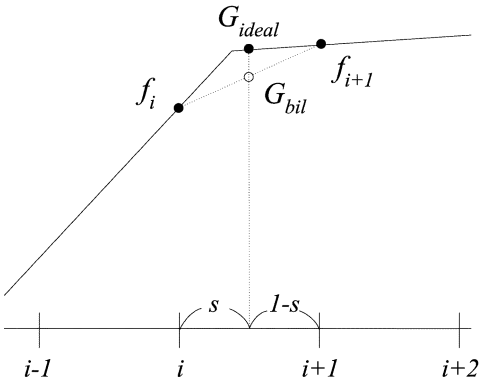

Fig. 2. One-dimensional bilinear interpolation.

the limitation of a 1-D bilinear interpolation. $G_{\rm bil}$ does not correctly represent the real point $G_{\rm ideal}$ in $[i, i+1]$ where the gradient changes abruptly. This phenomenon coincides with edges in 2-D images. Thus, in order to make $G_{\rm bil}$ closer to $G_{\rm ideal}$, the weights $(1-s)$ and s in $G_{\rm bil} = (1-s)f_i + sf_{i+1}$ need to be changed. If the weights $(1-s)$ and s are divided by each of the normalized local gradient of f_i and f_{i+1}, the weight for f_i becomes smaller and the weight for f_{i+1} becomes larger, since the normalized local gradient f_{i+1} is smaller than that of f_i. This makes $G_{\rm bil}$ larger, making $G_{\rm bil}$ closer to $G_{\rm ideal}$. Therefore, the weights should be determined by the ratio of the inverse gradients of f_i and f_{i+1}. From this motivation, this letter proposes two new interpolation methods using an inverse gradient to improve the perceptual performance of conventional interpolation operations.

Fig. 1 shows the definition of the four predefined masks from which the corresponding inverse gradient weights, H_l, H_r, V_u, and V_l are generated. For example, H_l is generated from the "Horizontal Left Mask," which is composed of the four neighbor pixels $f_{i-1,j}$, $f_{i,j}$, $f_{i-1,j+1}$, and $f_{i,j+1}$. The inverse gradient weights are defined as

$$\begin{aligned} H_l &= \frac{1}{\sqrt{1+\alpha\left(\text{abs}(f_{i,j}-f_{i-1,j})+\text{abs}(f_{i,j+1}-f_{i-1,j+1})\right)}} \\ H_r &= \frac{1}{\sqrt{1+\alpha\left(\text{abs}(f_{i+1,j}-f_{i+2,j})+\text{abs}(f_{i+1,j+1}-f_{i+2,j+1})\right)}} \\ V_u &= \frac{1}{\sqrt{1+\alpha\left(\text{abs}(f_{i,j}-f_{i,j-1})+\text{abs}(f_{i+1,j}-f_{i+1,j-1})\right)}} \\ V_l &= \frac{1}{\sqrt{1+\alpha\left(\text{abs}(f_{i,j+1}-f_{i,j+2})+\text{abs}(f_{i+1,j+1}-f_{i+1,j+2})\right)}} \end{aligned} \tag{3}$$

where α is the sharpness constant, which controls the sharpness of an image. Its value is bounded by [0,1], and if its value is 0, the inverse gradient weights become 1, which means the original bilinear interpolation. As α increases, the inverse gradient weights decrease below 1, which produces a sharper image. Using the inverse gradient weights, the adaptive bilinear interpolation can be defined as

$$\begin{aligned} G^A_{\rm bil}(x,y) = {} & w^v_0\left(w^h_0 f_{i,j} + w^h_1 f_{i+1,j}\right) \\ & + w^v_1\left(w^h_0 f_{i,j+1} + w^h_1 f_{i+1,j+1}\right) \end{aligned} \tag{4}$$

where $w^h_0 = (H_l(1-s)/D^h_{\rm bil})$, $w^h_1 = (H_r s/D^h_{\rm bil})$, $w^v_0 = (V_u(1-t)/D^v_{\rm bil})$, $w^v_1 = (V_l t/D^v_{\rm bil})$, $D^h_{\rm bil} = H_l(1-s) + H_r s$, and $D^v_{\rm bil} = V_u(1-t) + V_l t$.

III. A-Bicubic Interpolation

The 2-D bicubic interpolation function $G_{\rm bic}$ is [10]

$$G_{\rm bic}(x,y) = \sum_{n=-1}^{2}\sum_{m=-1}^{2} f_{i+m,j+n} P_{m+1}(s) P_{n+1}(t) \tag{5}$$

where $P_0(u) = (-u^3+2u^2-u)/2$, $P_1(u) = (3u^3-5u^2+2)/2$, $P_2(u) = (-3u^3+4u^2+u)/2$, $P_3(u) = (u^3-u^2)/2$, $s = x-x_i$, and $t = y-y_i$. Using the same inverse gradient weights in (3) as in the A-bilinear case, the adaptive bicubic interpolation can be defined as

$$G^A_{\rm bic}(x,y) = \sum_{n=-1}^{2}\sum_{m=-1}^{2} f_{i+m,j+n} w^h_{m+1}(s) w^v_{n+1}(t) \tag{6}$$

where $w^h_0(u) = (P_0(u)/D^h_{\rm bic})$, $w^h_1(u) = (H_l P_1(u)/D^h_{\rm bic})$, $w^h_2(u) = (H_r P_2(u)/D^h_{\rm bic})$, $w^h_3(u) = (P_3(u)/D^h_{\rm bic})$, $w^v_0(u) = (P_0(u)/D^v_{\rm bic})$, $w^v_1(u) = (V_u P_1(u)/D^v_{\rm bic})$, $w^v_2(u) = (V_l P_2(u)/D^v_{\rm bic})$, $w^v_3(u) = (P_3(u)/D^v_{\rm bic})$, $D^h_{\rm bic} = P_0(u) + H_l P_1(u) + H_r P_2(u) + P_3(u)$, and $D^v_{\rm bic} = P_0(u) + V_u P_1(u) + V_l P_2(u) + P_3(u)$.

IV. Determination of α

To determine the sharpness constant α, two objective measures are used. One is the PSNR and the other is the percentage edge error (PEE). Since the PSNR does not necessarily reflect the observer's visual perception of an error, the PEE is used together with the PSNR to measure perceptual errors. The PEE, defined in [11], scales the overall dissatisfaction of the viewer due to blocking artifact in JPEG, plus it is well suited to image magnification where the major artifact results from blurring. The PEE is defined by

$$\text{PEE} = \frac{\text{ES}_{\rm ORG} - \text{ES}_{\rm INTER}}{\text{ES}_{\rm ORG}} \times 100\% \tag{7}$$

where $\text{ES}_{\rm ORG}$ is the edge strength of the original image and $\text{ES}_{\rm INTER}$ is that of the interpolated image. The PEE measures how close the interpolated image details from the original image. Generally, in image interpolation, the PEE is positive, which means the interpolated image is over smoothed. Thus, a decrease in the PEE value is a strong indication of a reduction in the blurring effect. The procedure to calculate ES is identical to that used in [11].

For six images with a size of 256 × 256 and eight-bit gray level from MATLAB (cameraman, testpat1, ic), the USC image database (aerial, resolution chart), and EPFL Biomedical Imaging Group (lena), the optimum value of α was determined. The selection criteria was maximizing the PSNR, minimizing the PEE, and avoiding a negative PEE, which indicates large perceptual error. In the A-bilinear case, since α has no significant meaning, it was set at 1 for all the test images. Table I shows that no significant change occurred in the value of the PSNR and PEE in the A-bilinear case when changing α for

TABLE I
PSNR AND PEE VALUES OF THE A-BILINEAR AND A-BICUBIC FOR VARIOUS α FOR CAMERAMAN IMAGE

α	A-bilinear		A-bicubic	
	PSNR(dB)	PEE(%)	PSNR(dB)	PEE(%)
0.00	27.51	31.61	28.51	24.04
0.01	27.78	31.26	29.15	20.94
0.05	27.98	30.76	29.65	12.73
0.10	28.02	30.47	29.10	4.06
1.00	28.04	30.06	17.34	-99.64

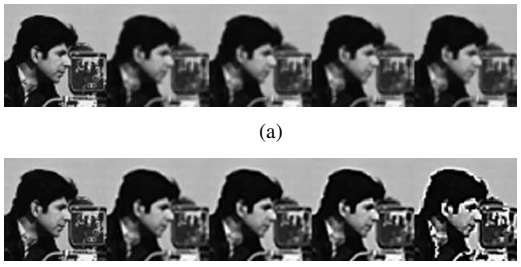

(a)

(b)

Fig. 3. Zooming on the selective region of cameraman shows the effect of α. (Left to right) Original image, interpolated images at $\alpha = 0.03$, $\alpha = 0.05$, $\alpha = 0.1$, and $\alpha = 0.5$. (a) A-bilinear case. (b) A-bicubic case.

the cameraman image. In contrast, in the A-bicubic case, α is valid within the range of [0, 0.1] and the optimum value is dependent on the image. Yet, in reality, any value within the range of [0.03, 0.07] showed a negligible perceptual degradation compared with the optimum value. Fig. 3 shows the effect of α on A-bilinear and A-bicubic interpolation. As α increased, the A-bilinear interpolation showed no perceptual difference, while the A-bicubic interpolation appeared sharper and noisier. This perceptual evidence from Fig. 3 coincided with the results of the PSNR and PEE.

So far the optimum value of α was only empirically determined for the A-bicubic case, thus the relationship between the values of α and the local gradients for the test images is also being investigated. The experimental results showed that the mean value of the inverse gradients, mean(H_l, H_r, V_u, V_l), obtained from the output images was approximately equal to 0.85 when the perceptually optimum value of α was applied to the original images. Therefore, such an iterative procedure was applied to obtain the perceptually optimum value of α for each interpolated pixel, where α was decreased when the local mean value of the inverse gradients was smaller than 0.85 and vice versa. Although this spatially adaptive α assignment approach is not yet totally complete, its current performance is presented in Section V.

V. SIMULATION RESULTS

Two objective measures were induced to study the effect of both random and structural errors on the interpolated images. The computer simulation was performed using the six test images previously referred to with a size of 256×256 that were lowpass filtered and subsampled to a size of 183×183, then the subsampled images were interpolated to the original image size. Thus, the corresponding MF r was 1.4. This approach is commonly used in the analysis of image interpolation algorithms

TABLE II
COMPARISON OF THE PERFORMANCE OF THE PROPOSED ALGORITHMS WITH CONVENTIONAL METHODS USING PSNR IN DECIBEL UNITS

image	Bil.	A-bil (α=1)	Bic.	A-bic (opti. α)	A-bic (adap. α)	cubic B-sp.
lena	31.62	32.31	32.85	33.64 (α=0.05)	33.35	32.77
camera-man	27.50	28.04	28.51	29.51 (α=0.07)	29.09	28.66
testpat1	29.68	31.88	32.10	33.40 (α=0.01)	31.47	31.61
ic	28.05	29.06	29.59	31.42 (α=0.03)	30.28	29.70
aerial	27.97	28.78	29.53	30.48 (α=0.05)	30.19	28.86
resolut-ion cha.	21.94	23.47	23.06	26.48 (α=0.07)	25.14	23.19

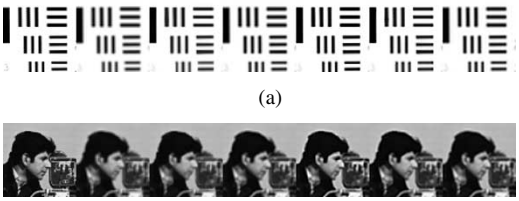

(a)

(b)

Fig. 4. Zooming on the selective regions of resolution chart and cameraman shows the results of various methods. (Left to right) Original image, interpolated images by bilinear, A-bilinear($\alpha = 1$), bicubic, A-bicubic($\alpha = 0.07$), A-bicubic(adaptive α), and cubic B-spline interpolation. (a) Resolution chart image. (b) Cameraman image.

[3], [9]. The MATLAB *imresize* function was used with the option of an 11-tap lowpass filter and bilinear subsampling.

The PSNR results for each interpolation algorithm are shown in Table II. The performance rankings were in the order of A-bicubic, A-bicubic (adaptive α), cubic B-sline, bicubic, A-bilinear, and bilinear interpolation, where A-bicubic (adaptive α) interpolation is the spatially adaptive α assignment method described in Section IV. The PSNR difference between A-bicubic and bicubic was 1 dB on average, except for the resolution chart image. A-bicubic (adaptive α) interpolation did exhibit some degradation compared to A-bicubic interpolation, yet still produced a better performance compared to bicubic and cubic B-sline interpolation. In particular, the proposed methods showed a better performance with black and white images, such as the resolution chart image. The improvement in the PSNR with A-bicubic interpolation was 3.4 dB, while A-bilinear interpolation was also superior to bicubic interpolation with an improvement in the PSNR of 0.4 dB. As regards perceptual quality, Fig. 4(a) demonstrates the superiority of the proposed methods.

The PEE results for each interpolation algorithm are shown in Table III. The results clearly show that the PEE for A-bicubic interpolation was very low compared with those for the other techniques. The main observation was that structural features were preserved and less affected by blurring in the A-bicubic case.

VI. CONCLUSION

This letter presents two adaptive interpolation methods based on applying an inverse gradient to conventional bilinear and

TABLE III
COMPARISON OF THE PERFORMANCE OF THE PROPOSED ALGORITHMS WITH CONVENTIONAL METHODS USING PEE IN PERCENTAGE UNITS

image	**Bil.**	**A-bil** (α=1)	**Bic.**	**A-bic** (opti. α)	**A-bic** (adap. α)	**cubic B-sp.**
lena	23.24	20.33	16.29	7.17 (α=0.05)	11.28	15.74
camera-man	31.61	30.11	24.04	9.07 (α=0.07)	19.67	23.83
testpat1	9.25	1.19	3.51	-0.76 (α=0.01)	-6.82	2.09
ic	19.39	17.38	12.33	4.12 (α=0.03)	7.20	11.46
aerial	30.02	26.67	22.30	9.88 (α=0.05)	16.09	19.57
resolut-ion cha.	23.58	24.50	18.71	9.96 (α=0.07)	15.65	18.15

bicubic interpolation. Due to the effective performance in edge regions, the proposed methods can be advantageously applied to synthetic images, including graphic and text images.

ACKNOWLEDGMENT

The authors express their sincere gratitude to the six anonymous reviewers for their valuable comments and suggestions.

REFERENCES

[1] H. Greenspan and C. H. Anderson, "Image enhancement by nonlinear extraction in frequency space," *Proc. SPIE*, vol. 2182, pp. 2–13, Feb. 1994.

[2] G.Guoping Qiu, "Interresolution look-up table for improved spatial magnification of image," *J. Visual Commun. Image Represent.*, vol. 2, pp. 360–373, 2000.

[3] W. K. Carey, D. B. Chung, and S. S. Hemami, "Regularity-preserving image interpolation," *IEEE Trans. Image Processing*, vol. 8, pp. 1293–1297, Sept. 1999.

[4] K. Jensen and D. Anastassiou, "Subpixel edge localization and the interpolation of still image," *IEEE Trans. Image Processing*, vol. 3, pp. 285–295, Mar. 1995.

[5] X. Li and M. T. Orchard, "New edge-directed interpolation," *IEEE Trans. Image Processing*, vol. 10, pp. 1521–1527, Oct. 2001.

[6] S. Carrato and L. Tenze, "A high quality 2× image interpolator," *IEEE Signal Processing Lett.*, vol. 7, pp. 132–134, June 2000.

[7] K. P. Hong, J. K. Paik, H. J. Kim, and C. H. Lee, "An edge-preserving image interpolation system for a digital camcoders," *IEEE Trans. Consumer Electron.*, vol. 42, pp. 279–284, Aug. 1996.

[8] C. Cai, T. H. Yu, and S. K. Mitra, "Saturation-based adaptive inverse gradient interpolation for Bayer pattern images," in *Proc. Inst. Elect. Eng. Vis. Image Signal Process.*, vol. 148, June 2001, pp. 202–208.

[9] A. Munoz, T. Blu, and M. Unser, "Least-squares image resizing using finite difference," *IEEE Trans. Image Processing*, vol. 10, pp. 1365–1378, Sept. 2001.

[10] R. G. Keys, "Cubic convolution interpolation for digital image processing," *IEEE Trans. Acoust., Speech, Signal Processing*, vol. ASSP-29, pp. 1153–1160, Dec. 1981.

[11] A. S. Al-Fahoum and A. M. Reza, "Combined edge crispiness and statistical differencing for deblocking JPEG compressed images," *IEEE Trans. Image Processing*, vol. 10, pp. 1288–1298, Sept. 2001.